SUPPLEMENTARY APPENDIX

Dominant negative *Gfi1b* mutations cause moderate thrombocytopenia and an impaired stress thrombopoiesis associated with mild erythropoietic abnormalities in mice

Hugues Beauchemin,[1] Peiman Shooshtharizadeh,[1] Jordan Pinder,[2] Graham Dellaire[2] and Tarik Möröy[1,3,4]

[1]Institut de Recherches Cliniques de Montréal, IRCM, Montréal, Quebec; [2]Departments of Pathology and Biochemistry and Molecular Biology, Dalhousie University, Halifax, Nova Scotia; [3]Département de Microbiologie, Infectiologie et Immunologie, Université de Montréal, Montréal, Quebec and [4]Division of Experimental Medicine, McGill University, Montréal, Quebec, Canada

 doi:10.3324/haematol.2019.222596

Received: March 20, 2019.

Accepted: November 21, 2019.

Pre-published: November 21, 2019.

Correspondence: *TARIK MÖRÖY* - tarik.moroy@ircm.qc.ca

Supplementary Methods

Mice

The generation of *Gfi1b*^{flox} and *Gfi1b*^{EGFP} knock-in mice were described previously.[1, 2] Hemizygote *Gfi1b*$^{WT/0}$ mice were obtained by breeding *Gfi1b*^{flox} females with an *EIIa-Cre* deleter male. The megakaryocyte-specific *Pf4-Cre* transgenic mouse strain C57BL/6-Tg(Pf4-icre)Q3Rsko/J (008535) and **the Cre-deleter strain** B6.FVB-Tg(EIIa-cre)C5379Lmgd/J (003724) were obtained from The Jackson Laboratory (Bar Harbor). All mice were housed under specific pathogen-free conditions.

CRISPR/Cas9-driven generation of Gfi1b mutant mouse lines

Gfi1b-specific gRNA targeting the 5th zinc finger was generated by hybridization of the two oligos CACCGGAGGTTGGAGCTCTGGCTGA and AAACTCAGCCAGAGCTCCAACCTCC and cloned into a BbsI-digested pX330-U6-Chimeric_BB-CBh-hSpCas9 vector, a gift from Feng Zhang (Addgene plasmid # 42230).[3] The vector was microinjected into (C57BL/6J × C3H/HeNHsd) F2 oocytes and the pups obtained were screened by sequencing to identify indel mutations in the 5th zinc finger of Gfi1b. Primers to amplify the region: GGCTGGGATCAAAGGTGTGG and AGGCGAGACACACTAAAGCA; and to sequence: CAGTAGCGAATGTGTGACAGG. Mice were backcossed for at least 6 generations on a pure C57BL/6J background.

Gfi1b expression analysis by qPCR

Total bone marrow was lineage depleted using the MojoSort^{TM} magnetic cell separation system using a biotin-conjugated B220, Mac-1, Gr-1, CD3, Ter119 antibody cocktail (BD Biosciences) and MojoSort™ Streptavidin Nanobeads (BioLegends). RNA was extracted using

the TriReagent (MRC) as per manufacturer's protocol. The total RNA was DNase I-treated and reverse transcribed with the SuperScript™ II Reverse Transcriptase (Invitrogen) using oligo(dT)$_{12\text{-}18}$ primers (Invitrogen). Quantitative real-time PCR was performed with PowerUP™ SYBR™ green master Mix (Applied Biosystems) with primer sets amplifying specifically exons 2 and 3 (GCACGCAGAAAAATGCCACG and CCGCTCCTGTTTGATTGTGTTC) or exons 5 and 6 (CCTGTGATGTCTGTGGCAAAACC and AGGGTGGATGAACGCTTGAAGG) of the murine *Gfi1b* gene, using *Rplp0* as housekeeping gene normalizer of input cDNA (primers: GAAACTGCTGCCTCACATCCG and GCTGGCACAGTGACCTGACACG). Triplicates were done for each PCR amplification that were carried out on a ViiA™ 7 Real-Time PCR System and analyzed with the QuantStudio™ Real-Time PCR Software v1.2 (Applied Biosystems).

Cloning of Gfi1b mutant cDNA

CD41^{+} cells were purified from total bone marrow from *Gfi1b*$^{WT/del2}$, *Gfi1b*$^{WT/del7}$, *Gfi1b*$^{WT/ins4}$ and *Pf4-cre*:*Gfi1b*$^{WT/flox}$ mice with the MojoSort™ magnetic cell separation system using biotin-conjugated anti-CD41 (BioLegend) and MojoSort™ Streptavidin Nanobeads (BioLegends). RNA was extracted and revers transcribed as described in the previous section. The *Gfi1b* cDNAs were PCR-amplified with the Phusion® High-Fidelity DNA Polymerase (New England Biolabs) using the following primers: AACAGGTACCGACAGTGTGGAGGTTCG and AACAGCATGCCAGAAAGGCCCGAACTG. The amplicons were digested with KpnI and SphI restriction enzymes (New England Biolabs) and cloned into the KpnI/SphI-digested mammalian expression vector pLexm, which was a gift from Edith Yvonne Jones (Addgene plasmid # 99844).[4]

Transfection of Gfi1b expression vectors and luciferase assay.

In transfection experiments, 50,000 HEK-293T cells (ATCC # CRL-11268) were seeded in 24-well plates, and co-transfected 24 hours later with 500 ng of the luciferase reporter pGL3 vector (Promega) containing the human Gfi1b promoter[5] and pLexm-*Gfi1b*^{DN} expression vectors along with 40 ng of EF4-β-gal expression vector using Lipofectamin 2000 (Invitrogen) for 48 hours according to manufacturer's protocol. Cells were then lysed in 100 µl of Reporter lysis buffer ($(MgCO_3)\cdot 4\ Mg(OH)_2\cdot 5H_2O$ (1.07 mM); $MgSO_4$ (2.67 mM); EDTA (0.1 mM); firefly D-luciferin (470 µM; Bioshop); coenzyme A (270 µM; Bioshop); DTT (33.3 µM); ATP (530 µM)). 30 µl of lysate were transferred into a 96-well luciferase plate and luminescence measured on a GloMax® 96 Microplate Luminometer (Promega) and 6X loading buffer was added to the another 30 µl of lysate and boiled 5 min for further Western blot analysis.

Western blot

The protein lysate from the transfection assay was loaded on a 10 % SDS-PAGE and transferred to PVDF Immobilon-P membrane (Millipore) at 4° C. After blocking in PBS/0.1% Tween 20 and 5% milk for 1 hour at room temperature, membranes were incubated with the anti-GFI1B (clone B-7; Santa Cruz) mouse monoclonal antibody or the anti-Glucose 6 Phosphate Dehydrogenase G6PD (ab993; abcam) rabbit polyclonal antibody for 1 hour. Membranes were then washed in PBS/0.1% Tween 20 and incubated with either a chicken anti-mouse HRP-conjugated (sc-2962; Santa Cruz).and the chicken anti-rabbit HRP-conjugated (sc-2963; Santa Cruz) secondary antibody for 1 hour. Bands were visualized using the SuperSignal West Dura kit (Thermo Scientific) according to the manufacturer's instructions.

Transmission electron microscopy

Platelet for electron microscopy were pelleted and prepared according published protocol with some modifications.[6] Briefly, the blood drawn by hearty puncture from four mice per genotype was pooled and the plasma was prefixed with 0.05% glutaraldehyde (Sigma-Aldrich) for 15 min at 37°C. Platelet pellets were the fixed with 3% glutaraldehyde in White's saline at 23°C for 1h followed by a post-fixation with 1% osmium tetroxide (Electron Microscopy Sciences) in White's saline at 4°C for 1h. Pellets where then serially dehydrated with increasing concentration of ethanol and propylene oxide (Sigma-Aldrich) and embedded in Epoxy Embedding Medium (Sigma-Aldrich). Blocks were thin-sectioned by ultramicrotomy and imaged on a Tecnai G^2 Spirit BioTwin 120 kV Cryo-TEM (FEI Company) equipped with an Ultrascan 4000 4k x 4k CCD Camera 895 (Gatan) located at the Facility for Electron Microscopy Research at McGill University.

Blood smears

Blood smears were prepared from heparinized fresh blood drawn from the mice mandibular vein and stained with StainRITE May-Grünwald/Giemsa (MGG; Polysciences, inc) as per manufacturer's protocol.

Flow cytometry analysis of the bone marrow

Bone marrow was harvested from two femora in RPMI w/o phenol red (Wisent) supplemented with 10 % Fetalgro® bovine growth serum (RMBIO) and filtered in a 100 μm cell strainer. Cells were first labeled with a biotin-conjugated (CD3, B220, Gr1, CD11b and Ter119 (BD Biosciences), CD19, CD8, CD4 and NK1.1 (BioLegend) and Il7R (eBioscience)) lineage cocktail, then with BV605-conjugated streptavidin, BV421-conjugated anti-cKit, FITC-conjugated anti-Sca1, APC/Cy7-conjugated anti-CD16/32, Alexa Fluor 647-conjugated anti-

CD105, Pacific Blue-conjugated anti-CD150 (all from BioLegend) and Alexa Fluor 700-conjugated anti-CD9 (Novus) to detect LT-HSCs ($Lin^-CD41^{low}CD9^{low}CD150^+CD105^+$), MKPs ($Lin^-CD16/32^-Sca1^-cKit^+CD41^{high}$), MKs ($CD41^{high}CD9^{high}$), PreCFUe ($Lin^-cKit^+Sca1^-CD16/32^-CD105^+CD150^+$) and PreMegE ($Lin^-cKit^+Sca1^-CD16/32^-CD105^-CD150^+$), or with Alexa Fluor 647-conjugated anti-Ter119 and PE-conjugated anti-CD71 (BioLegend) to detect erythroid precursors. Acquisition was done on a SA3800 Spectral Analyzer (Sony) and analyzed with FlowJo v.10.5 (FlowJo LLC).

Erythropoietic and thrombopoietic stresses induction

To induce an acute but transient hemolytic anemia, mice were injected were injected intraperitoneally for two consecutive days with Phenylhydrazine (Sigma-Aldrich) at 60 μg/g bodyweight.[7] In the experiment where mice were followed over time, from day two onward, 25 uL of peripheral blood were taken every two days with heparinized microcapillaries to assess red blood cell loss/recovery by measuring the hematocrit. To induce transient acute thrombocytopenia, mice were injected intravenously with anti-GPIba antibody (clone R300; Emfret Analytics) at 2μg/g bodyweight.[8] In the experiment where mice were followed over time, every day, 10 uL of peripheral blood were taken with heparinized microcapillaries to assess platelet loss and recovery by quantitative FACS. To induce thrombocytosis, mice were injected once intraperitoneally with 500 ng of the TPO mimetic romiplostim (AMGEN).

Statistical methods.

Values are expressed as means ± standard deviations (SD) or as medians when the distribution did not pass the D'Agostino and Pearson omnibus normality test. When two groups were compared, an unpaired Student's *t*-test to compare the means, or the Mann-Whitney test to

compare the medians were used. When three or more groups were compared, a one-way analysis of variance (ANOVA) with Tukey's multiple comparison tests (samples with equal variance) or a Welsh's ANOVA test with either Holm-Sidak's or Games-Howell's multiple comparisons tests (samples with unequal variance) were used to compare means. Alternatively, the Kruskal-Wallis test and Dunn's multiple comparisons tests were used to compare medians. The Fisher's exact test and χ^2 test were used to assess mendelian transmission. All *P* values were calculated using Prism software v.8.3.0 (GraphPad) and in all statistical tests, a $P < 0.05$ was considered significant.

Supplementary References

1. Khandanpour C, Sharif-Askari E, Vassen L, et al. Evidence that growth factor independence 1b regulates dormancy and peripheral blood mobilization of hematopoietic stem cells. Blood. 2010;116(24):5149-5161.
2. Vassen L, Okayama T, Moroy T. Gfi1b:green fluorescent protein knock-in mice reveal a dynamic expression pattern of Gfi1b during hematopoiesis that is largely complementary to Gfi1. Blood. 2007;109(6):2356-2364.
3. Cong L, Ran FA, Cox D, et al. Multiplex genome engineering using CRISPR/Cas systems. Science. 2013;339(6121):819-823.
4. Aricescu AR, Lu W, Jones EY. A time- and cost-efficient system for high-level protein production in mammalian cells. Acta Crystallogr D Biol Crystallogr. 2006;62(Pt 10):1243-1250.
5. Vassen L, Fiolka K, Mahlmann S, Moroy T. Direct transcriptional repression of the genes encoding the zinc-finger proteins Gfi1b and Gfi1 by Gfi1b. Nucleic Acids Res. 2005;33(3):987-998.
6. White JG. Electron microscopy methods for studying platelet structure and function. Methods Mol Biol. 2004;272(47-63.
7. Hara H, Ogawa M. Erthropoietic precursors in mice with phenylhydrazine-induced anemia. Am J Hematol. 1976;1(4):453-458.
8. Nieswandt B, Bergmeier W, Rackebrandt K, Gessner JE, Zirngibl H. Identification of critical antigen-specific mechanisms in the development of immune thrombocytopenic purpura in mice. Blood. 2000;96(7):2520-2527.

Supplementary table 1: Mosaicism in founders

Founder	Carried alleles (≈%)	sequence
357	WT (50%)	AAAGCCTTCAGCCAGAGCTC
	11822 Ins4 fs1 (15%)	AAAGCCTTCAgaaaGCCAGAGCTC
	11820 del2 fs1(30%)	AAAGCCTT..GCCAGAGCTC
	11822 G→C(5%)	AAAGCCTTCAcCCAGAGCTC
361	WT (75%)	AAAGCCTTCAGCCAGAGCTC
	11818 del7 fs2 (25%)	AAAGCC.......AGAGCTC
395	WT (33%)	AAAGCCTTCAGCCAGAGCTC
	11821 del4 fs2 (33%)	AAAGCCTTC....AGAGCTC
	11822 Ins7 fs1	AAAGCCTTCAtaaccaaGCCAGAGCTC
399	WT (50%)	AAAGCCTTCAGCCAGAGCTC
	11818 del7 fs2 (50%)	AAAGCC.......AGAGCTC
408	WT (80%)	AAAGCCTTCAGCCAGAGCTC
	11818 del7 fs2(20%)	AAAGCC.......AGAGCTC
414	WT (50%)	AAAGCCTTCAGCCAGAGCTC
	11820 del2 (25%)	AAAGCCTT..GCCAGAGCTC
	11822 ins4 fs2 (25%)	AAAGCCTTCAccaaGCCAGAGCTC

***Gfi1b*-S286T** (11822 G→C)
EKPHKCQVCGKAFTQSSNLITHSRKHTGFKPFSCELCTKGFQRKVDLRRHRESQHNLK*

***Gfi1b*-S286fsX309** (ins7)
EKPHKCQVCGKAFITKPELQPHHPQPQAHRLQAVQL*

***Gfi1b*-S286fsX335** (del4)
EKPHKCQVCGKAFRAPTSSPTAASTQASSRSAVSCAPRASSARWTCDVTVRVNTISSETVGRLL*

***Gfi1b*-S286fsX308** (ins4 v.2)
EKPHKCQVCGKAFTKPELQPHHPQPQAHRLQAVQL*

Supplementary Figure 1: Resulting C-terminus of the proteins produced by the mutants that were not transmitted to progeny and found in founders 357 (11822 G→C), 395 (ins7 and del4) and 414 (ins4 v.2). As in Figure 1, the 5th and 6th zinc fingers are highlighted in yellow and the substituted amino-acids, as well as the extraneous peptide sequences generated by the frameshifts, are identified in red.

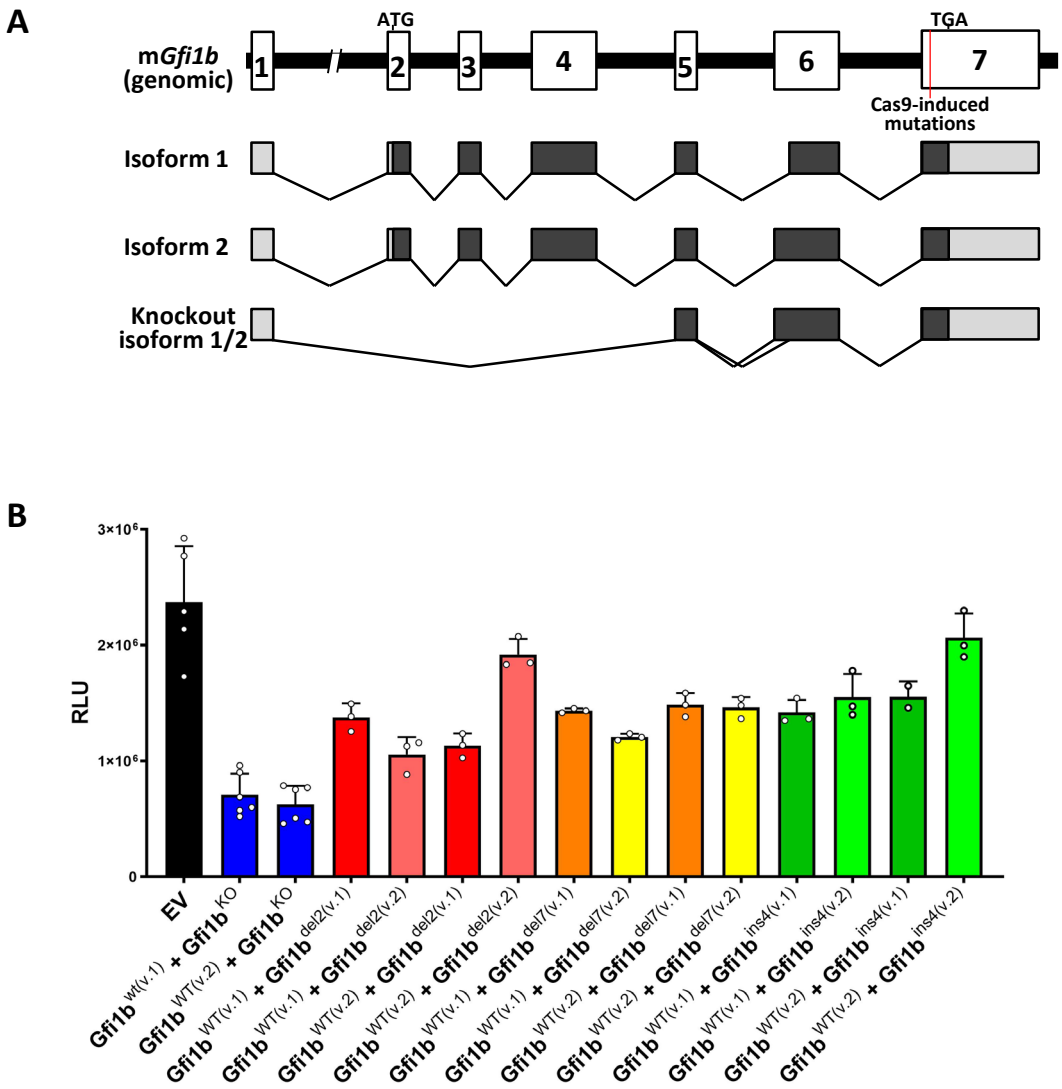

Supplementary Figure 2: Expression and cloning of murine *Gfi1b*. (A) Schematic representation of the two major splice variants of the mouse Gfi1b gene (isoforms 1 and 2) caused by an alternative spicing site within exon 6. In the *Gfi1b* knockout animals, the exons 2 to 4 are lost leading to a mRNA lacking an ORF and therefore not producing a protein. (B) Uncombined results of the luciferase assay (Figure 2E) showing the capacity of both isoforms of the three mutants to inhibit repression by either WT GFI1B isoforms.

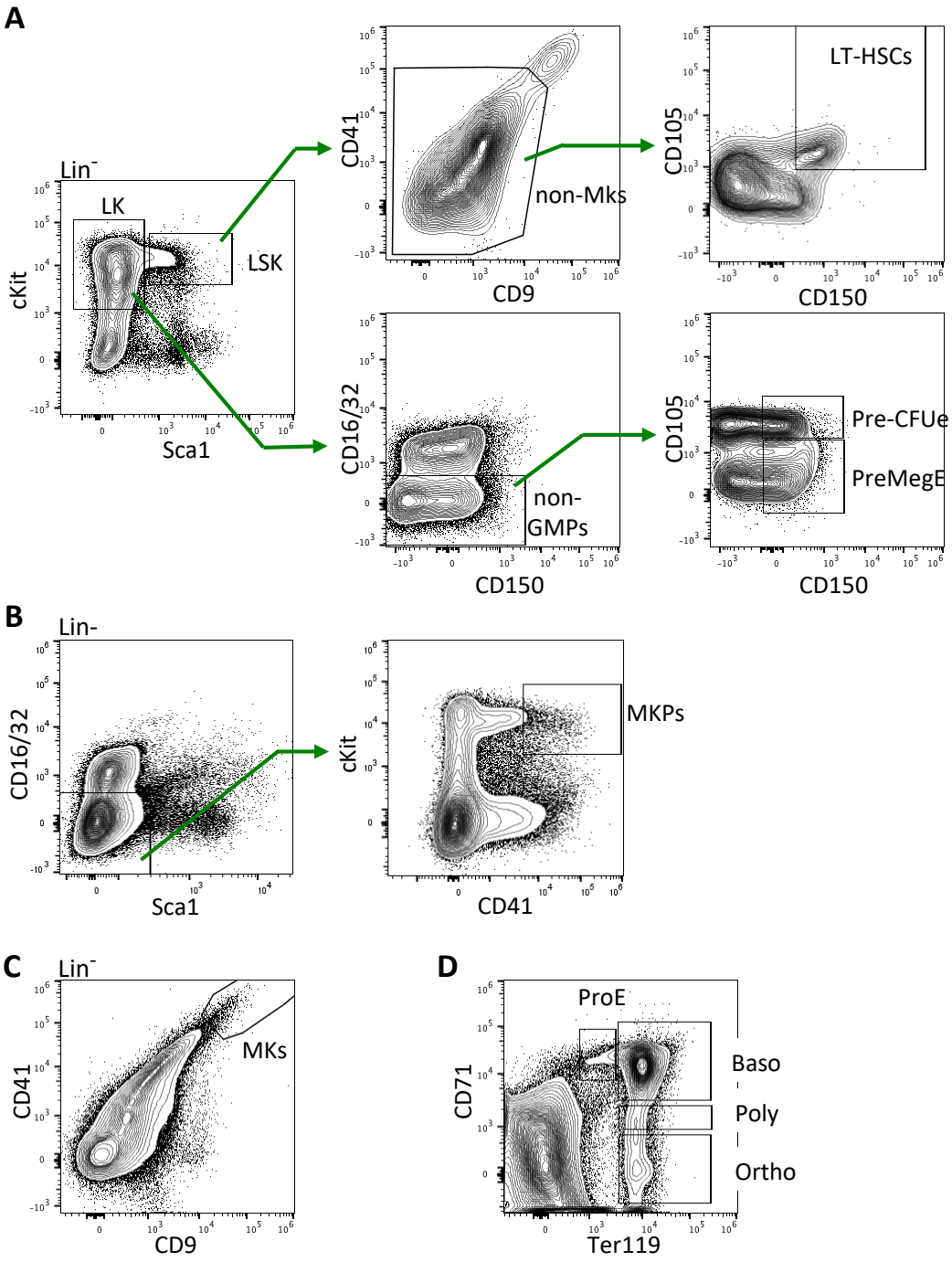

Supplementary Figure 3: Gating strategy for bone marrow analysis by FACS to identify (A) long term hematopoietic stem cells (LT-HSCs; Lin$^-$cKit$^+$Sca1$^+$CD41^{low}CD9^{low}CD105$^+$CD150$^+$), PreMegE (Lin$^-$cKit$^+$Sca1$^-$CD16/32$^-$CD105$^-$CD150$^+$) and PreCFUe (Lin$^-$cKit$^+$Sca1$^-$CD16/32$^-$CD105$^+$CD150$^+$), (B) megakaryocyte progenitors (MKPs; Lin$^-$cKit$^+$Sca1$^-$CD16/32$^-$CD41^{high}), (C) Megakaryocytes (MKs; Lin$^-$CD41^{high}CD9^{high}) and (D) proerythroblasts (ProE; CD71^{high}Ter119^{low}), basophilic erythroblasts (Baso; CD71^{high}Ter119$^+$), polychromatophilic erythroblasts (Poly; CD71^{medium}Ter119$^+$) and orthochomatophilic erythroblasts (Ortho; CD71$^-$Ter119$^+$).

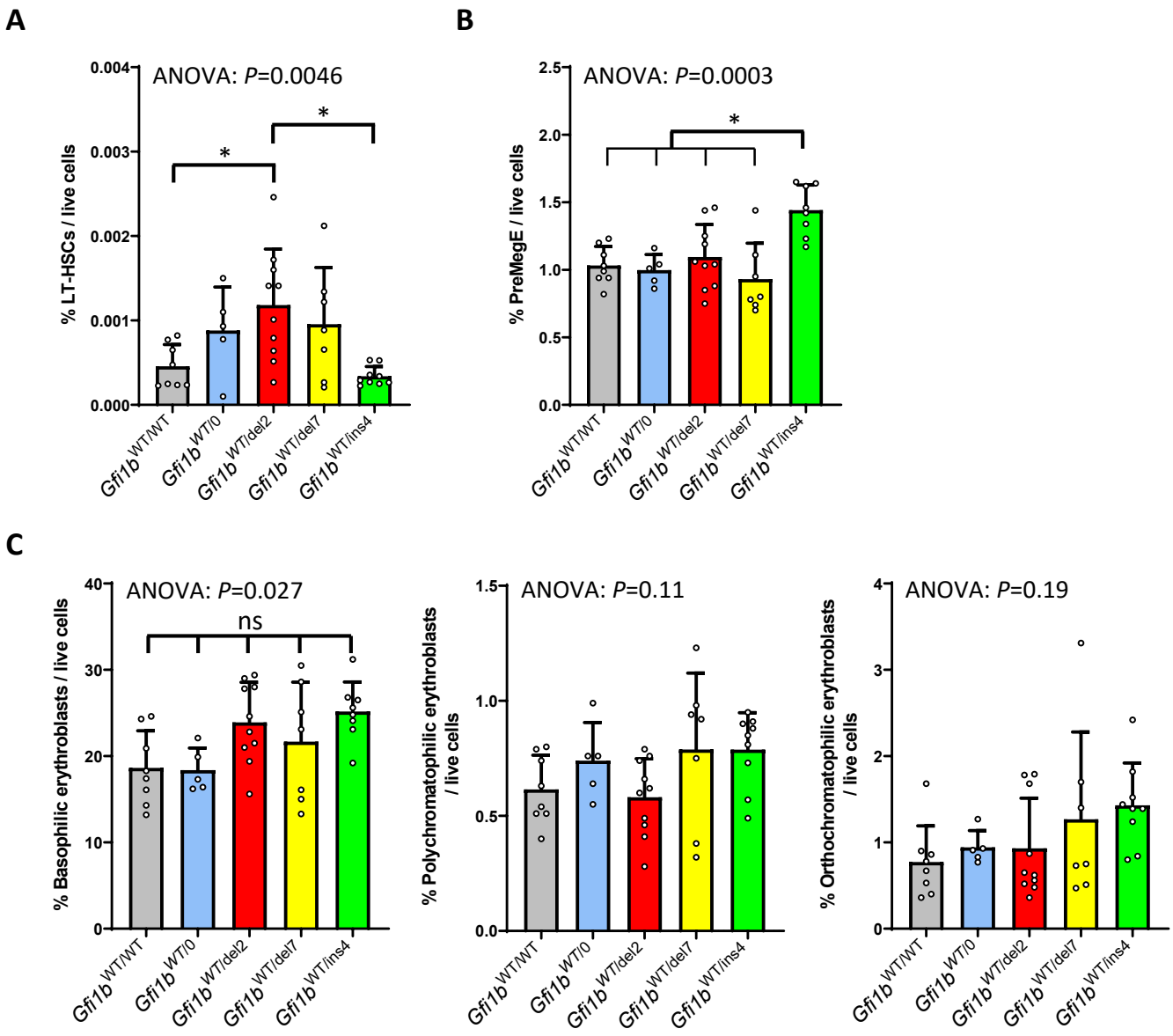

Supplementary Figure 4: Quantification of the FACS analysis of bone marrow at steady state (Figure 4) for (A) LT-HSCs, (B) PreMegE, (C) basophilic erythroblasts, polychromatophilic erythroblasts and orthochromatophilic erythroblasts. All results are reported as mean ± SD and significance was calculated by ANOVA tests and, when significance was found, followed by a Holm-Sidak's multiple comparisons test comparing the mean of each column with the mean of every other column. The full results of the Holm-Sidak's tests in panels (A) and (B) are presented in the Online Supplementary Table S8 and S9 respectively and summarized here with * = significant. Although the ANOVA gave a significant *P*-value for the basophilic erythroblasts (C), the Holm-Sidak's tests found no statistical significance.

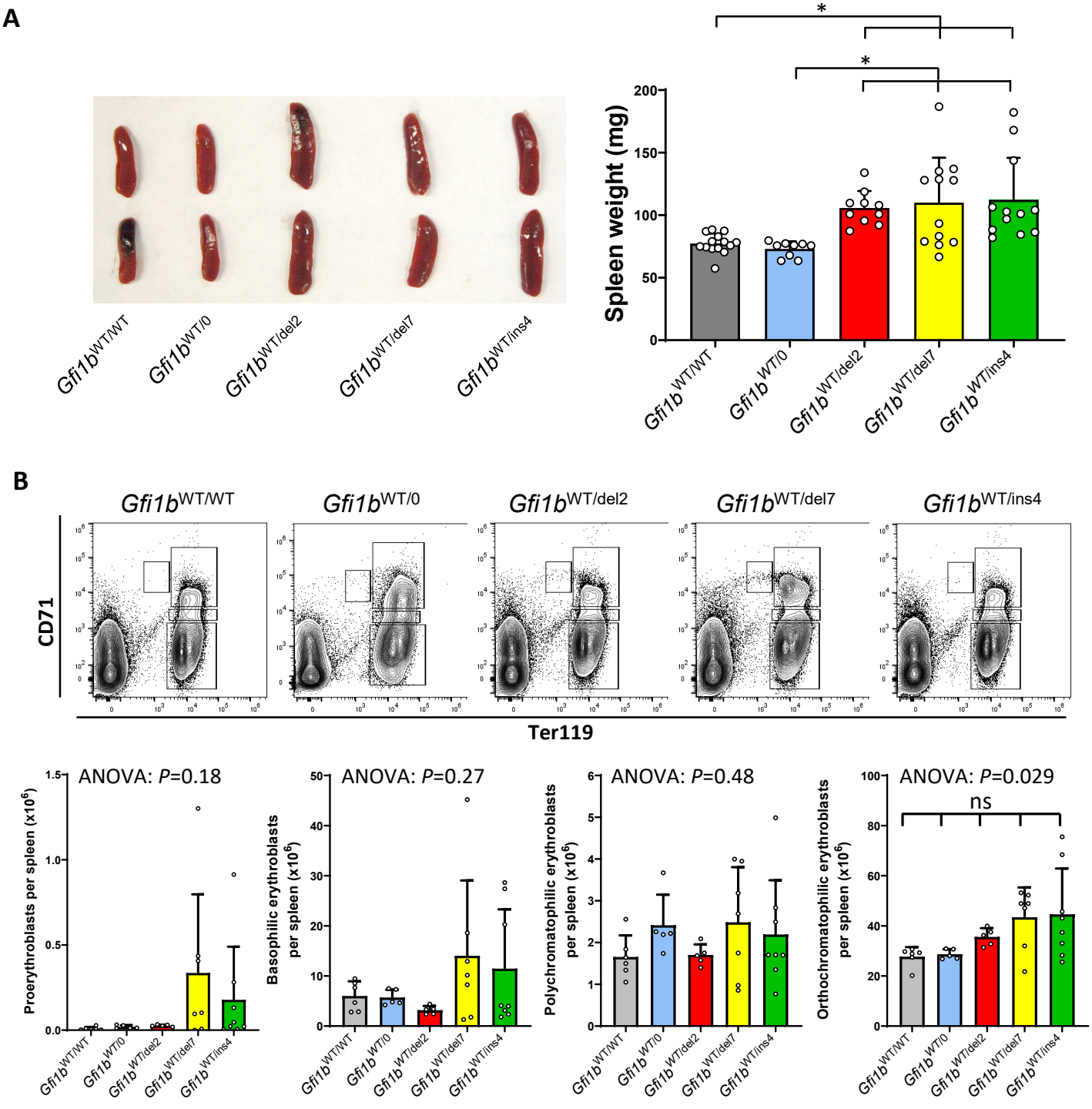

Supplementary Figure 5: Spleen characterization at steady state. (A) Moderate spleen enlargement in 6-week old females Gfi1b-DN compared to Gfi1b$^{WT/WT}$ and Gfi1b$^{WT/0}$ hemizygous females of the same age. (B) FACS analysis of Spleen for proerythroblasts, basophilic, polychromatophilic and orthochromatophilic erythroblasts. All results are reported as mean of total cells per spleen ± SD and significance was calculated by ANOVA and, when significance was found, followed by a Holm-Sidak's multiple comparisons test comparing the mean of each column with the mean of every other column. The full results of the Holm-Sidak's tests in panels (A) are presented in the Online Supplementary Tables S10 and summarized here with * = significant. Although the ANOVA gave a significant *P*-value for the orthochromatophilic erythroblasts (B), the Holm-Sidak's tests found no statistical significance.

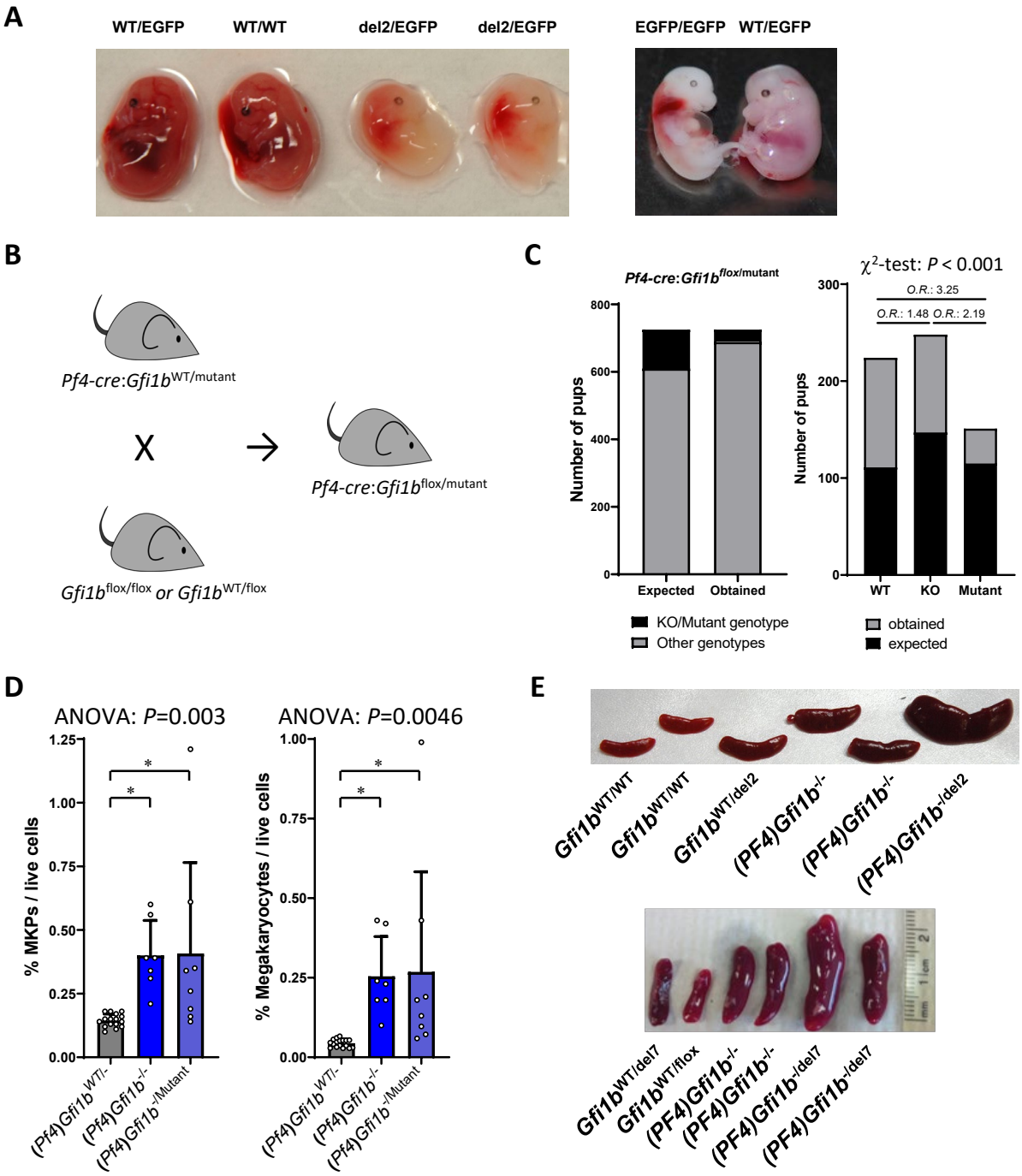

Supplementary Figure 6: (A) Fetuses from a cross between *Gfi1b*$^{WT/del2}$ x *Gfi1b*$^{WT/EGFP}$ (left) or *Gfi1b*$^{WT/EGFP}$ x *Gfi1b*$^{WT/EGFP}$ (right) with their *Gfi1b* genotype. (B) Breeding scheme used to produce *Pf4-cre*:*Gfi1b*$^{flox/mutant}$. (C) Total number of pups obtained with the (KO/DN) or other genotypes and compared with the amount expected based on a perfect mendelian transmission (left). Comparison of the obtained number of pups with the proper genotype over the number expected for *Pf4-Cre*:*Gfi1b*$^{WT/WT}$ (WT), *Pf4-Cre*:*Gfi1b*$^{flox/flox}$ (KO; from a crossing *Pf4-Cre*:*Gfi1b*$^{flox/wt}$ X *Gfi1b*$^{flox/WT}$), or *Pf4-Cre*:*Gfi1b*$^{flox/mutant}$ (Mutant) mice (right). (D) Quantification of the FACS analysis of bone marrow at steady state for MKPs and Mks. Results are reported as mean ± SD and significance was calculated using one-way ANOVA tests followed by Holm-Sidak's multiple comparisons test comparing the mean of each column with the mean of every other column: * = adjusted *P* value < 0.05. (E) Severe splenomegaly observed in *Pf4-Cre*:*Gfi1b*$^{flox/del2}$ and *Pf4-Cre:Gfi1b*$^{flox/del7}$ mice compared to *Pf4-Cre*:*Gfi1b*$^{flox/flox}$, and *Gfi1b*$^{WT/del2}$ of *Gfi1b*$^{WT/del7}$ and *Gfi1b*$^{WT/WT}$.

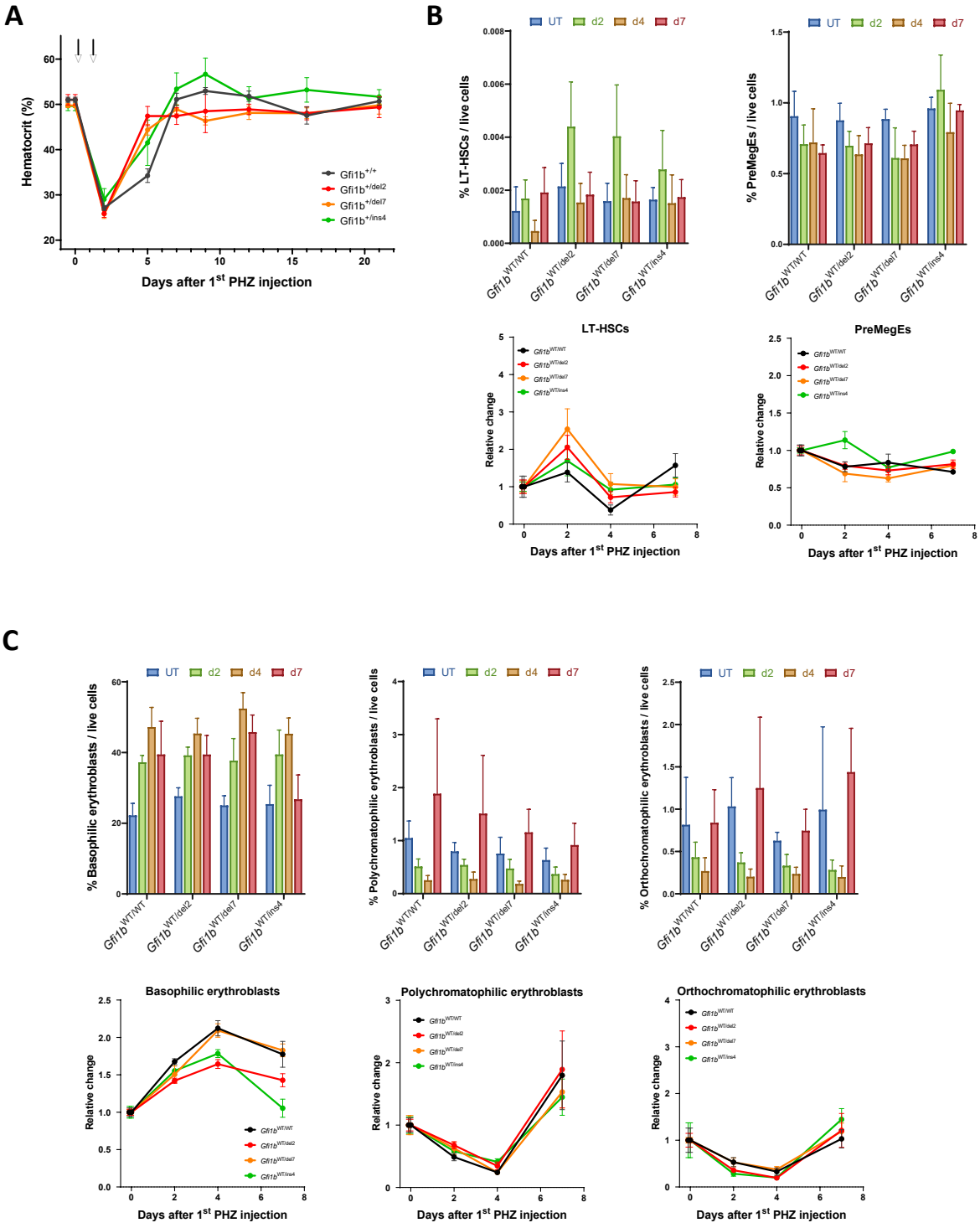

Supplementary Figure 7: (A) Time course analysis of the response to PHZ-induced hemolytic anemia. 5 to 10 mice for each genotype were injected twice with PHZ and minimally bled every 2-3 days to measure hematocrit. Results are reported as mean ± SD of the percentage of RBC volume / blood volume. (B-C) Analysis by flow cytometry of the bone marrow from the mice treated as described in Figure 6. Quantification of LT-HSCs and PreMegE (B) or basophilic, polychromatophilic and orthochromatophilic erythroblasts (C) and reported as mean ± SD of % of cells per live cells (top) or as change relative to day 0 (bottom).

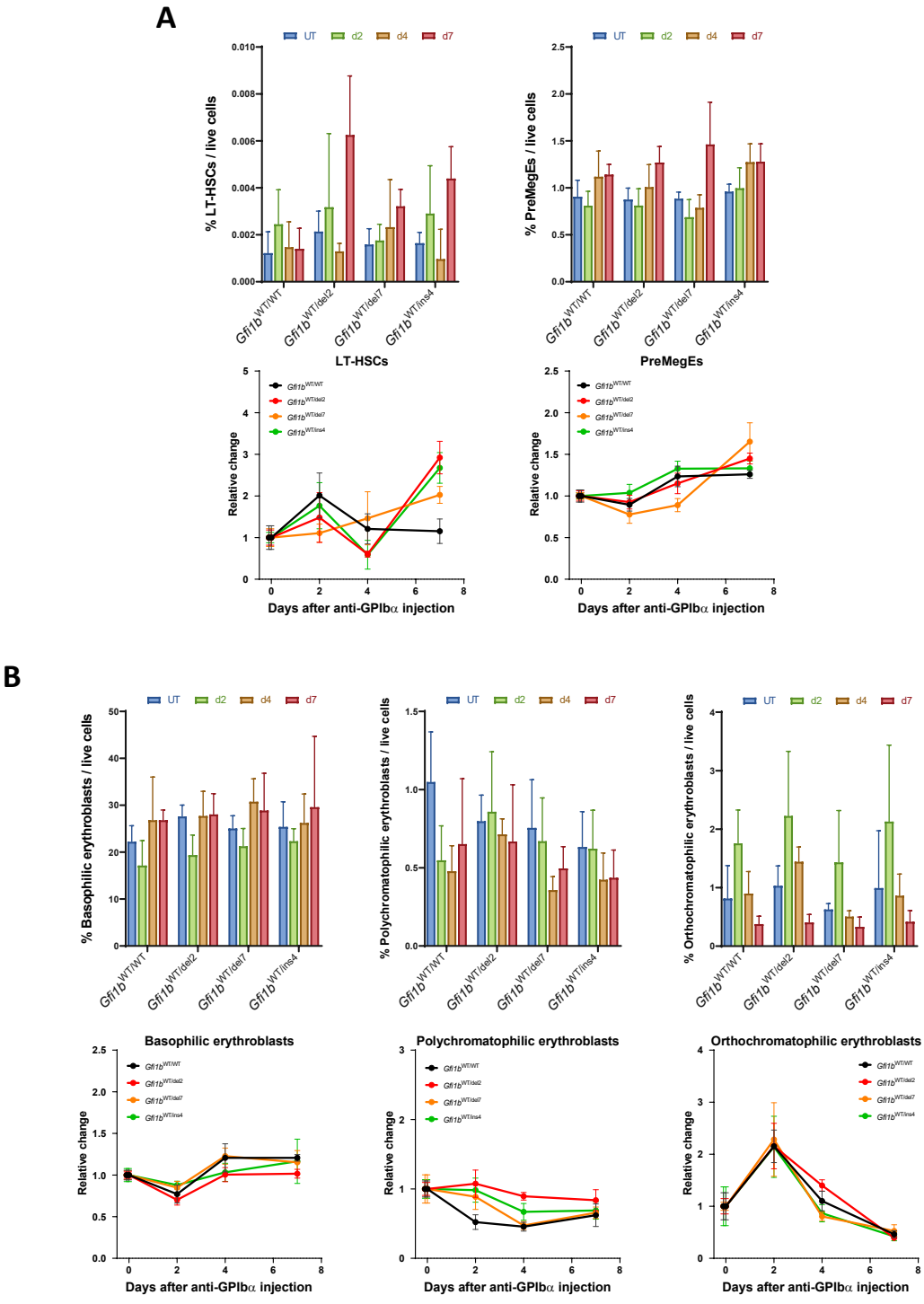

Supplementary Figure 8: Quantification by flow cytometry of bone marrow from the anti-*GPIba* antibody-treated mice (Figure 7) for (A) LT-HSCs and PreMegE, or (B) basophilic, polychromatophilic and orthochromatophilic erythroblasts and reported as mean ± SD of % of cells per live cells (top) or as change relative to day 0 (bottom).

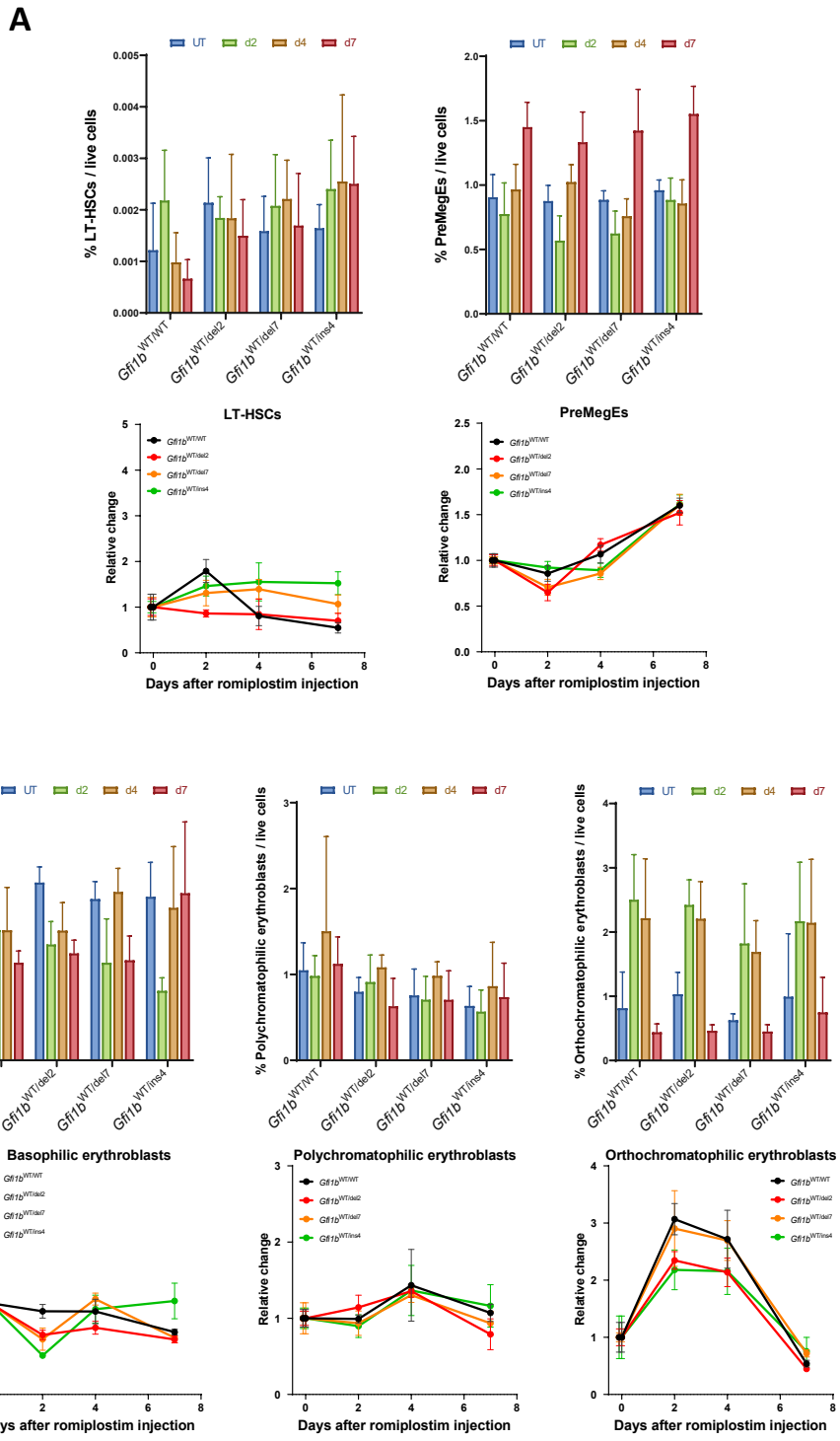

Supplementary Figure 9: Quantification by flow cytometry of bone marrow from the romiplostim-treated mice from (Figure 8) for (A) LT-HSCs and PreMegE, or (B) basophilic, polychromatophilic and orthochromatophilic erythroblasts and reported as mean ± SD of % of cells per live cells (top) or as change relative to day 0 (bottom).

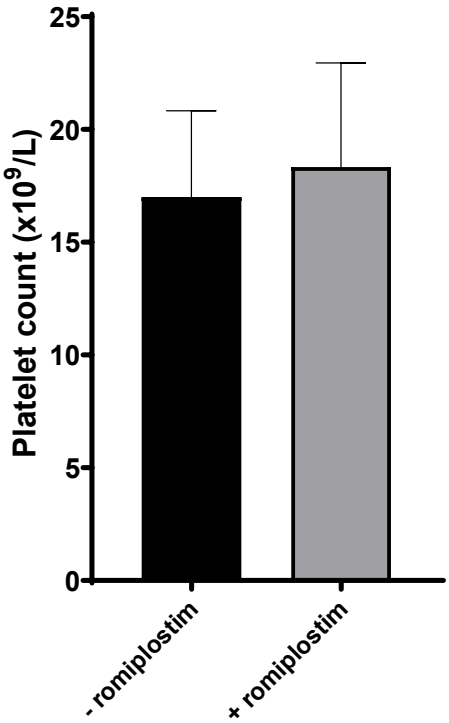

Supplementary Figure 10: *Pf4-cre*:*Gfi1b*$^{flox/flox}$ mice were injected with 500 ng of romiplostim and platelet count was measured on an Advia apparatus 7 days after injection, and compared to mice that did not receive romiplostim. Statistical significance was calculated using a Student's *t*-test: $P = 0.99$.

Supplementary Table 2: *P* values for the Dunn's multiple comparisons test (Figure 2D)

Repression of luciferase activity

Kruskal-Wallis test: *P* <0.0001

Dunn's multiple comparisons test	Mean rank diff.	Significant?	Summary	Adjusted P Value
EV vs. GFI1B$^{KO(v.1)}$	-7.862	No	ns	>0.9999
EV vs. GFI1B$^{KO(v.2)}$	9.331	No	ns	>0.9999
EV vs. hGFI1B$^{(v.1)}$	48.33	No	ns	0.2897
EV vs. GFI1B$^{WT(v.1)}$	62.96	Yes	**	0.0059
EV vs. GFI1B$^{WT(v.2)}$	63.68	Yes	**	0.0064
EV vs. GFI1B$^{del2(v.1)}$	-11.67	No	ns	>0.9999
EV vs. GFI1B$^{del2(v.2)}$	5.6	No	ns	>0.9999
EV vs. GFI1B$^{del7(v.1)}$	-13.67	No	ns	>0.9999
EV vs. GFI1B$^{del7(v.2)}$	8.645	No	ns	>0.9999
EV vs. GFI1B$^{ins4(v.1)}$	-9.956	No	ns	>0.9999
EV vs. GFI1B$^{ins4(v.2)}$	15.6	No	ns	>0.9999
GFI1B$^{KO(v.1)}$ vs. GFI1B$^{KO(v.2)}$	17.19	No	ns	>0.9999
GFI1B$^{KO(v.1)}$ vs. hGFI1B$^{(v.1)}$	56.19	Yes	*	0.0272
GFI1B$^{KO(v.1)}$ vs. GFI1B$^{WT(v.1)}$	70.82	Yes	***	0.0001
GFI1B$^{KO(v.1)}$ vs. GFI1B$^{WT(v.2)}$	71.54	Yes	***	0.0002
GFI1B$^{KO(v.1)}$ vs. GFI1B$^{del2(v.1)}$	-3.811	No	ns	>0.9999
GFI1B$^{KO(v.1)}$ vs. GFI1B$^{del2(v.2)}$	13.46	No	ns	>0.9999
GFI1B$^{KO(v.1)}$ vs. GFI1B$^{del7(v.1)}$	-5.811	No	ns	>0.9999
GFI1B$^{KO(v.1)}$ vs. GFI1B$^{del7(v.2)}$	16.51	No	ns	>0.9999
GFI1B$^{KO(v.1)}$ vs. GFI1B$^{ins4(v.1)}$	-2.094	No	ns	>0.9999
GFI1B$^{KO(v.1)}$ vs. GFI1B$^{ins4(v.2)}$	23.46	No	ns	>0.9999
GFI1B$^{KO(v.2)}$ vs. hGFI1B$^{(v.1)}$	39	No	ns	0.9385
GFI1B$^{KO(v.2)}$ vs. GFI1B$^{WT(v.1)}$	53.63	Yes	*	0.0222
GFI1B$^{KO(v.2)}$ vs. GFI1B$^{WT(v.2)}$	54.35	Yes	*	0.0237
GFI1B$^{KO(v.2)}$ vs. GFI1B$^{del2(v.1)}$	-21	No	ns	>0.9999
GFI1B$^{KO(v.2)}$ vs. GFI1B$^{del2(v.2)}$	-3.731	No	ns	>0.9999
GFI1B$^{KO(v.2)}$ vs. GFI1B$^{del7(v.1)}$	-23	No	ns	>0.9999
GFI1B$^{KO(v.2)}$ vs. GFI1B$^{del7(v.2)}$	-0.6853	No	ns	>0.9999
GFI1B$^{KO(v.2)}$ vs. GFI1B$^{ins4(v.1)}$	-19.29	No	ns	>0.9999
GFI1B$^{KO(v.2)}$ vs. GFI1B$^{ins4(v.2)}$	6.269	No	ns	>0.9999
hGFI1B$^{(v.1)}$ vs. GFI1B$^{WT(v.1)}$	14.63	No	ns	>0.9999
hGFI1B$^{(v.1)}$ vs. GFI1B$^{WT(v.2)}$	15.35	No	ns	>0.9999
hGFI1B$^{(v.1)}$ vs. GFI1B$^{del2(v.1)}$	-60	Yes	*	0.0191
hGFI1B$^{(v.1)}$ vs. GFI1B$^{del2(v.2)}$	-42.73	No	ns	0.6505
hGFI1B$^{(v.1)}$ vs. GFI1B$^{del7(v.1)}$	-62	Yes	*	0.0119
hGFI1B$^{(v.1)}$ vs. GFI1B$^{del7(v.2)}$	-39.68	No	ns	>0.9999
hGFI1B$^{(v.1)}$ vs. GFI1B$^{ins4(v.1)}$	-58.28	No	ns	0.0553

hGFI1B$^{(v.1)}$ vs. GFI1B$^{ins4(v.2)}$	-32.73	No	ns	>0.9999
GFI1B$^{WT(v.1)}$ vs. GFI1B$^{WT(v.2)}$	0.7198	No	ns	>0.9999
GFI1B$^{WT(v.1)}$ vs. GFI1B$^{del2(v.1)}$	-74.63	Yes	***	0.0001
GFI1B$^{WT(v.1)}$ vs. GFI1B$^{del2(v.2)}$	-57.36	Yes	*	0.0162
GFI1B$^{WT(v.1)}$ vs. GFI1B$^{del7(v.1)}$	-76.63	Yes	****	<0.0001
GFI1B$^{WT(v.1)}$ vs. GFI1B$^{del7(v.2)}$	-54.31	Yes	*	0.0341
GFI1B$^{WT(v.1)}$ vs. GFI1B$^{ins4(v.1)}$	-72.91	Yes	***	0.0007
GFI1B$^{WT(v.1)}$ vs. GFI1B$^{ins4(v.2)}$	-47.36	No	ns	0.5555
GFI1B$^{WT(v.2)}$ vs. GFI1B$^{del2(v.1)}$	-75.35	Yes	***	0.0001
GFI1B$^{WT(v.2)}$ vs. GFI1B$^{del2(v.2)}$	-58.08	Yes	*	0.0172
GFI1B$^{WT(v.2)}$ vs. GFI1B$^{del7(v.1)}$	-77.35	Yes	****	<0.0001
GFI1B$^{WT(v.2)}$ vs. GFI1B$^{del7(v.2)}$	-55.03	Yes	*	0.0357
GFI1B$^{WT(v.2)}$ vs. GFI1B$^{ins4(v.1)}$	-73.63	Yes	***	0.0008
GFI1B$^{WT(v.2)}$ vs. GFI1B$^{ins4(v.2)}$	-48.08	No	ns	0.5451
GFI1B$^{del2(v.1)}$ vs. GFI1B$^{del2(v.2)}$	17.27	No	ns	>0.9999
GFI1B$^{del2(v.1)}$ vs. GFI1B$^{del7(v.1)}$	-2	No	ns	>0.9999
GFI1B$^{del2(v.1)}$ vs. GFI1B$^{del7(v.2)}$	20.32	No	ns	>0.9999
GFI1B$^{del2(v.1)}$ vs. GFI1B$^{ins4(v.1)}$	1.717	No	ns	>0.9999
GFI1B$^{del2(v.1)}$ vs. GFI1B$^{ins4(v.2)}$	27.27	No	ns	>0.9999
GFI1B$^{del2(v.2)}$ vs. GFI1B$^{del7(v.1)}$	-19.27	No	ns	>0.9999
GFI1B$^{del2(v.2)}$ vs. GFI1B$^{del7(v.2)}$	3.045	No	ns	>0.9999
GFI1B$^{del2(v.2)}$ vs. GFI1B$^{ins4(v.1)}$	-15.56	No	ns	>0.9999
GFI1B$^{del2(v.2)}$ vs. GFI1B$^{ins4(v.2)}$	10	No	ns	>0.9999
GFI1B$^{del7(v.1)}$ vs. GFI1B$^{del7(v.2)}$	22.32	No	ns	>0.9999
GFI1B$^{del7(v.1)}$ vs. GFI1B$^{ins4(v.1)}$	3.717	No	ns	>0.9999
GFI1B$^{del7(v.1)}$ vs. GFI1B$^{ins4(v.2)}$	29.27	No	ns	>0.9999
GFI1B$^{del7(v.2)}$ vs. GFI1B$^{ins4(v.1)}$	-18.6	No	ns	>0.9999
GFI1B$^{del7(v.2)}$ vs. GFI1B$^{ins4(v.2)}$	6.955	No	ns	>0.9999
GFI1B$^{ins4(v.1)}$ vs. GFI1B$^{ins4(v.2)}$	25.56	No	ns	>0.9999

Supplementary Table 3: *P* values for the Dunn's multiple comparisons test (Figure 2E)

Dominant-negative function of Gfi1b^{DN}

Kruskal-Wallis test: *P* <0.0001

Dunn's multiple comparisons test	Mean rank diff.	Significant?	Summary	Adjusted P Value
EV vs. Gfi1b^{WT} + Gfi1b^{KO}	41.53	Yes	****	<0.0001
EV vs. Gfi1b^{WT} + Gfi1b^{del2}	22.12	No	ns	0.0611
EV vs. Gfi1b^{WT} + Gfi1b^{del7}	19.62	No	ns	0.1502
EV vs. Gfi1b^{WT} + Gfi1b^{ins4}	11.75	No	ns	>0.9999
Gfi1b^{WT} + Gfi1b^{KO} vs. Gfi1b^{WT} + Gfi1b^{del2}	-19.42	Yes	*	0.017
Gfi1b^{WT} + Gfi1b^{KO} vs. Gfi1b^{WT} + Gfi1b^{del7}	-21.92	Yes	**	0.004
Gfi1b^{WT} + Gfi1b^{KO} vs. Gfi1b^{WT} + Gfi1b^{ins4}	-29.79	Yes	****	<0.0001
Gfi1b^{WT} + Gfi1b^{del2} vs. Gfi1b^{WT} + Gfi1b^{del7}	-2.5	No	ns	>0.9999
Gfi1b^{WT} + Gfi1b^{del2} vs. Gfi1b^{WT} + Gfi1b^{ins4}	-10.37	No	ns	>0.9999
Gfi1b^{WT} + Gfi1b^{del7} vs. Gfi1b^{WT} + Gfi1b^{ins4}	-7.871	No	ns	>0.9999

Supplementary Table 4: *P* values for the Dunnett's T3 multiple comparisons test (Figure 3A)

Platelet count

Brown-Forsythe ANOVA: *P* <0.0001

Dunnett's T3 multiple comparisons test	Mean Diff.	Significant?	Summary	Adjusted P Value
Gfi1b$^{WT/WT}$ vs. *Gfi1b*$^{WT/0}$	53.57	No	ns	0.5925
Gfi1b$^{WT/WT}$ vs. *Gfi1b*$^{WT/del2}$	280.7	Yes	****	<0.0001
Gfi1b$^{WT/WT}$ vs. *Gfi1b*$^{WT/del7}$	215	Yes	****	<0.0001
Gfi1b$^{WT/WT}$ vs. *Gfi1b*$^{WT/ins4}$	314.5	Yes	****	<0.0001
Gfi1b$^{WT/0}$ vs. *Gfi1b*$^{WT/del2}$	227.1	Yes	****	<0.0001
Gfi1b$^{WT/0}$ vs. *Gfi1b*$^{WT/del7}$	161.5	Yes	**	0.0011
Gfi1b$^{WT/0}$ vs. *Gfi1b*$^{WT/ins4}$	260.9	Yes	***	0.0001
Gfi1b$^{WT/del2}$ vs. *Gfi1b*$^{WT/del7}$	-65.61	No	ns	0.8984
Gfi1b$^{WT/del2}$ vs. *Gfi1b*$^{WT/ins4}$	33.85	No	ns	0.9998
Gfi1b$^{WT/del7}$ vs. *Gfi1b*$^{WT/ins4}$	99.45	No	ns	0.5951

Supplementary Table 5: *P* values for the Holm-Sidak's multiple comparisons test (Figure 3B)

Platelet CD41 MFI

ANOVA: *P*=0.0023

Holm-Sidak's multiple comparisons test	Mean Diff.	Significant?	Summary	Adjusted P Value
Gfi1b$^{WT/WT}$ vs. *Gfi1b*$^{WT/del2}$	-135.8	Yes	*	0.0338
Gfi1b$^{WT/WT}$ vs. *Gfi1b*$^{WT/del7}$	-138.8	Yes	**	0.003
Gfi1b$^{WT/WT}$ vs. *Gfi1b*$^{WT/ins4}$	-128.6	Yes	*	0.0171
Gfi1b$^{WT/del2}$ vs. *Gfi1b*$^{WT/del7}$	-3	No	ns	0.9909
Gfi1b$^{WT/del2}$ vs. *Gfi1b*$^{WT/ins4}$	7.143	No	ns	0.9909
Gfi1b$^{WT/del7}$ vs. *Gfi1b*$^{WT/ins4}$	10.14	No	ns	0.9909

Supplementary Table 6: *P* values for the Holm-Sidak's multiple comparisons test (Figure 4B)

MKPs

ANOVA: *P* <0.0001

Holm-Sidak's multiple comparisons test	Mean Diff.	Significant?	Summary	Adjusted P Value
Gfi1b$^{WT/WT}$ vs. *Gfi1b*$^{WT/del2}$	-0.1484	Yes	****	<0.0001
Gfi1b$^{WT/WT}$ vs. *Gfi1b*$^{WT/del7}$	-0.09566	Yes	*	0.014
Gfi1b$^{WT/WT}$ vs. *Gfi1b*$^{WT/ins4}$	-0.1069	Yes	**	0.0033
Gfi1b$^{WT/WT}$ vs. *Gfi1b*$^{WT/0}$	0.01063	No	ns	0.9059
Gfi1b$^{WT/del2}$ vs. *Gfi1b*$^{WT/del7}$	0.05271	No	ns	0.2376
Gfi1b$^{WT/del2}$ vs. *Gfi1b*$^{WT/ins4}$	0.04144	No	ns	0.3135
Gfi1b$^{WT/del2}$ vs. *Gfi1b*$^{WT/0}$	0.159	Yes	****	<0.0001
Gfi1b$^{WT/del7}$ vs. *Gfi1b*$^{WT/ins4}$	-0.01127	No	ns	0.9059
Gfi1b$^{WT/del7}$ vs. *Gfi1b*$^{WT/0}$	0.1063	Yes	*	0.014
Gfi1b$^{WT/ins4}$ vs. *Gfi1b*$^{WT/0}$	0.1176	Yes	**	0.0046

Megakaryocytes

ANOVA: *P* <0.0001

Holm-Sidak's multiple comparisons test	Mean Diff.	Significant?	Summary	Adjusted P Value
Gfi1b$^{WT/WT}$ vs. *Gfi1b*$^{WT/del2}$	-0.09203	Yes	****	<0.0001
Gfi1b$^{WT/WT}$ vs. *Gfi1b*$^{WT/del7}$	-0.06034	Yes	**	0.0022
Gfi1b$^{WT/WT}$ vs. *Gfi1b*$^{WT/ins4}$	-0.06418	Yes	***	0.0006
Gfi1b$^{WT/WT}$ vs. *Gfi1b*$^{WT/0}$	0.02158	No	ns	0.3835
Gfi1b$^{WT/del2}$ vs. *Gfi1b*$^{WT/del7}$	0.03169	No	ns	0.147
Gfi1b$^{WT/del2}$ vs. *Gfi1b*$^{WT/ins4}$	0.02784	No	ns	0.147
Gfi1b$^{WT/del2}$ vs. *Gfi1b*$^{WT/0}$	0.1136	Yes	****	<0.0001
Gfi1b$^{WT/del7}$ vs. *Gfi1b*$^{WT/ins4}$	-0.003841	No	ns	0.8006
Gfi1b$^{WT/del7}$ vs. *Gfi1b*$^{WT/0}$	0.08191	Yes	***	0.0003
Gfi1b$^{WT/ins4}$ vs. *Gfi1b*$^{WT/0}$	0.08576	Yes	****	<0.0001

Supplementary Table 7: *P* values for the Holm-Sidak's multiple comparisons test (Figure 4C)

PreCFUe

ANOVA: *P* <0.0001

Holm-Sidak's multiple comparisons test	Mean Diff.	Significant?	Summary	Adjusted P Value
Gfi1b$^{WT/WT}$ vs. *Gfi1b*$^{WT/del2}$	-1.457	Yes	****	<0.0001
Gfi1b$^{WT/WT}$ vs. *Gfi1b*$^{WT/del7}$	-0.7618	Yes	**	0.0096
Gfi1b$^{WT/WT}$ vs. *Gfi1b*$^{WT/ins4}$	-0.6275	Yes	*	0.0275
Gfi1b$^{WT/WT}$ vs. *Gfi1b*$^{WT/0}$	-0.0115	No	ns	0.962
Gfi1b$^{WT/del2}$ vs. *Gfi1b*$^{WT/del7}$	0.6947	Yes	*	0.0123
Gfi1b$^{WT/del2}$ vs. *Gfi1b*$^{WT/ins4}$	0.829	Yes	**	0.0028
Gfi1b$^{WT/del2}$ vs. *Gfi1b*$^{WT/0}$	1.445	Yes	****	<0.0001
Gfi1b$^{WT/del7}$ vs. *Gfi1b*$^{WT/ins4}$	0.1343	No	ns	0.8012
Gfi1b$^{WT/del7}$ vs. *Gfi1b*$^{WT/0}$	0.7503	Yes	*	0.0227
Gfi1b$^{WT/ins4}$ vs. *Gfi1b*$^{WT/0}$	0.616	No	ns	0.0519

Proerythroblasts

ANOVA: *P* <0.0001

Holm-Sidak's multiple comparisons test	Mean Diff.	Significant?	Summary	Adjusted P Value
Gfi1b$^{WT/WT}$ vs. *Gfi1b*$^{WT/del2}$	-0.4194	Yes	****	<0.0001
Gfi1b$^{WT/WT}$ vs. *Gfi1b*$^{WT/del7}$	-0.4152	Yes	****	<0.0001
Gfi1b$^{WT/WT}$ vs. *Gfi1b*$^{WT/ins4}$	-0.2824	Yes	****	<0.0001
Gfi1b$^{WT/WT}$ vs. *Gfi1b*$^{WT/0}$	-0.01778	No	ns	0.9316
Gfi1b$^{WT/del2}$ vs. *Gfi1b*$^{WT/del7}$	0.004143	No	ns	0.9316
Gfi1b$^{WT/del2}$ vs. *Gfi1b*$^{WT/ins4}$	0.137	Yes	*	0.0293
Gfi1b$^{WT/del2}$ vs. *Gfi1b*$^{WT/0}$	0.4016	Yes	****	<0.0001
Gfi1b$^{WT/del7}$ vs. *Gfi1b*$^{WT/ins4}$	0.1329	Yes	*	0.0439
Gfi1b$^{WT/del7}$ vs. *Gfi1b*$^{WT/0}$	0.3975	Yes	****	<0.0001
Gfi1b$^{WT/ins4}$ vs. *Gfi1b*$^{WT/0}$	0.2646	Yes	***	0.0002

Supplementary Table 8: *P* values for the Holm-Sidak's multiple comparisons test (Supplementary Figure S4A)

LT-HSCs

ANOVA: *P*=0.0046

Holm-Sidak's multiple comparisons test	Mean Diff.	Significant?	Summary	Adjusted P Value
Gfi1b$^{WT/WT}$ vs. *Gfi1b*$^{WT/del2}$	-0.0007246	Yes	*	0.0348
Gfi1b$^{WT/WT}$ vs. *Gfi1b*$^{WT/del7}$	-0.0004984	No	ns	0.3364
Gfi1b$^{WT/WT}$ vs. *Gfi1b*$^{WT/ins4}$	0.0001188	No	ns	0.8584
Gfi1b$^{WT/WT}$ vs. *Gfi1b*$^{WT/0}$	-0.0004239	No	ns	0.5328
Gfi1b$^{WT/del2}$ vs. *Gfi1b*$^{WT/del7}$	0.0002262	No	ns	0.7366
Gfi1b$^{WT/del2}$ vs. *Gfi1b*$^{WT/ins4}$	0.0008434	Yes	**	0.0072
Gfi1b$^{WT/del2}$ vs. *Gfi1b*$^{WT/0}$	0.0003007	No	ns	0.722
Gfi1b$^{WT/del7}$ vs. *Gfi1b*$^{WT/ins4}$	0.0006172	No	ns	0.1367
Gfi1b$^{WT/del7}$ vs. *Gfi1b*$^{WT/0}$	0.00007449	No	ns	0.8584
Gfi1b$^{WT/ins4}$ vs. *Gfi1b*$^{WT/0}$	-0.0005427	No	ns	0.3364

Supplementary Table 9: *P* values for the Holm-Sidak's multiple comparisons test (Supplementary Figure S4B)

PreMegE

ANOVA: *P*=0.0003

Holm-Sidak's multiple comparisons test	Mean Diff.	Significant?	Summary	Adjusted P Value
Gfi1b$^{WT/WT}$ vs. *Gfi1b*$^{WT/del2}$	-0.0625	No	ns	0.8915
Gfi1b$^{WT/WT}$ vs. *Gfi1b*$^{WT/del7}$	0.1011	No	ns	0.8801
Gfi1b$^{WT/WT}$ vs. *Gfi1b*$^{WT/ins4}$	-0.4088	Yes	**	0.003
Gfi1b$^{WT/WT}$ vs. *Gfi1b*$^{WT/0}$	0.0345	No	ns	0.8915
Gfi1b$^{WT/del2}$ vs. *Gfi1b*$^{WT/del7}$	0.1636	No	ns	0.5145
Gfi1b$^{WT/del2}$ vs. *Gfi1b*$^{WT/ins4}$	-0.3463	Yes	**	0.0077
Gfi1b$^{WT/del2}$ vs. *Gfi1b*$^{WT/0}$	0.097	No	ns	0.8801
Gfi1b$^{WT/del7}$ vs. *Gfi1b*$^{WT/ins4}$	-0.5098	Yes	***	0.0003
Gfi1b$^{WT/del7}$ vs. *Gfi1b*$^{WT/0}$	-0.06657	No	ns	0.8915
Gfi1b$^{WT/ins4}$ vs. *Gfi1b*$^{WT/0}$	0.4433	Yes	**	0.0046

Supplementary Table 10: *P* values for the Holm-Sidak's multiple comparisons test (Supplementary Figure S5A)

Spleen weight

ANOVA: *P*=0.0001

Holm-Sidak's multiple comparisons test	Mean Diff.	Significant?	Summary	Adjusted P Value
Gfi1b$^{WT/WT}$ vs. *Gfi1b*$^{WT/0}$	4.334	No	ns	0.9647
Gfi1b$^{WT/WT}$ vs. *Gfi1b*$^{WT/del2}$	-28.45	Yes	*	0.0283
Gfi1b$^{WT/WT}$ vs. *Gfi1b*$^{WT/del7}$	-32.75	Yes	**	0.007
Gfi1b$^{WT/WT}$ vs. *Gfi1b*$^{WT/ins4}$	-34.94	Yes	**	0.0046
Gfi1b$^{WT/0}$ vs. *Gfi1b*$^{WT/del2}$	-32.78	Yes	*	0.025
Gfi1b$^{WT/0}$ vs. *Gfi1b*$^{WT/del7}$	-37.09	Yes	**	0.007
Gfi1b$^{WT/0}$ vs. *Gfi1b*$^{WT/ins4}$	-39.28	Yes	**	0.0046
Gfi1b$^{WT/del2}$ vs. *Gfi1b*$^{WT/del7}$	-4.307	No	ns	0.9647
Gfi1b$^{WT/del2}$ vs. *Gfi1b*$^{WT/ins4}$	-6.497	No	ns	0.95
Gfi1b$^{WT/del7}$ vs. *Gfi1b*$^{WT/ins4}$	-2.189	No	ns	0.9647

Uncropped blots (from figure 2)

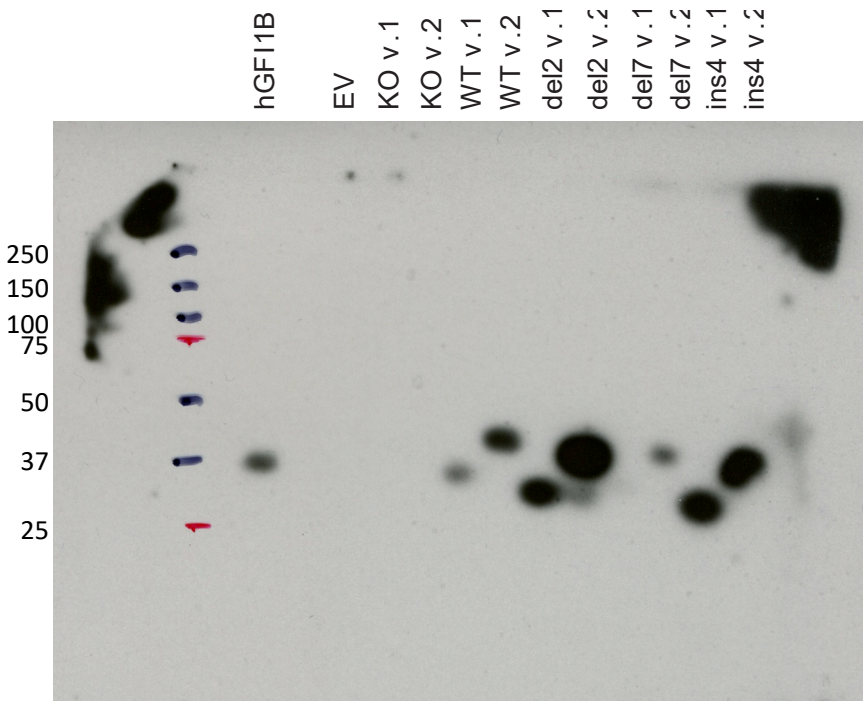

Gfi1b

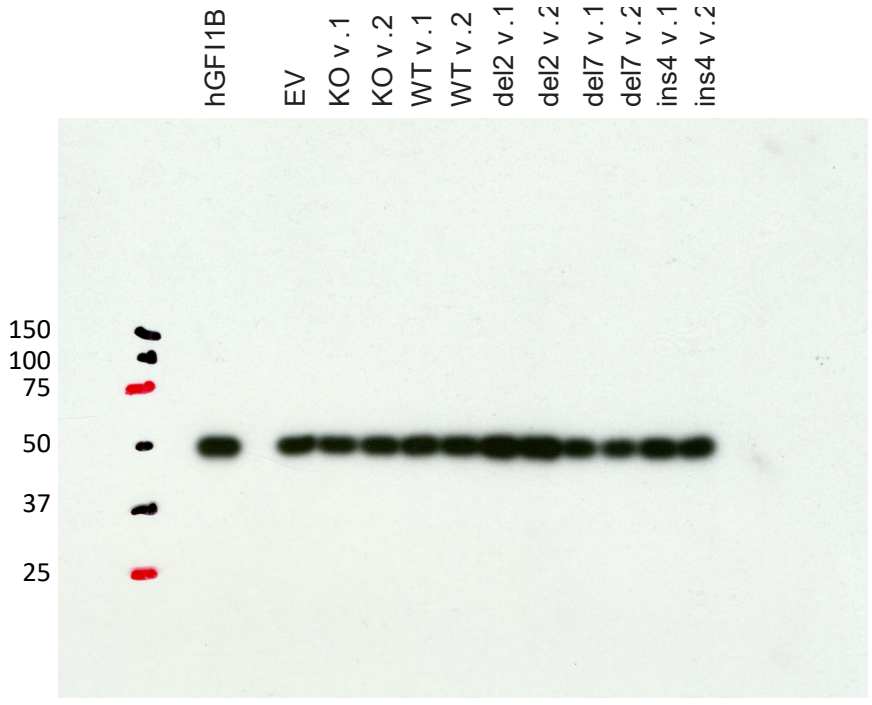

G6PD